12.3 LARGE-EDDY SIMULATION OF FLOW FIELD AND POLLUTANT TRANSPORT INSIDE URBAN STREET CANYONS WITH HIGH ASPECTS RATIOS

Xian-Xiang Li, Chun-Ho Liu, Dennis Y.C. Leung*
Department of Mechanical Engineering, The University of Hong Kong, Hong Kong, China

1. INTRODUCTION

A "street canyon", which constitutes the basic geometric unit of urban areas, is a relatively narrow street in-between buildings that line up continuously along both sides. It has a distinct climate where micro-scale meteorological processes dominate (Oke, 1988) and the ventilation and pollutant removal are solely through the roof level. Poor air quality is often encountered near the pedestrian level inside these street canyons since the surrounding tall buildings block the approaching wind, which in turns causes recirculations of air pollutant inside street canyons (DePaul and Sheih, 1986; Nakamura and Oke, 1988).

The wind flow inside street canyons is characterized by the building-height-to-street-width (aspect) ratio (AR, h/b, where h is the building height and b the street width). As a function of the AR, the flow regime inside street canyons can be classified into isolated roughness flow, wake interference flow and skimming flow (Oke, 1988). The behavior of a passive and inert gaseous pollutant is closely related to the flow pattern inside street canyons. Therefore, using field measurement, laboratory experiment, or computational fluid dynamics (CFD), many studies have been performed in the past three decades. Owing to the rapid development of computer capacity and sophisticated numerical models, CFD has become a useful tool to explore the processes occurring in street canyons in details. The recent advancement of using CFD in street-canyon pollution problems is reviewed elsewhere (Li et al. 2006).

The early CFD studies mainly utilized the two-equation k−ε turbulence model to handle the turbulent flow and pollutant dispersion in street canyons. For a street canyon of low AR (<1), a primary recirculation was identified (Lee and Park, 1994; Johnson and Hunter, 1995; Baik and Kim, 1999; Huang et al., 2000; Li et al., 2005). For street canyons of higher AR (1.5–2.7), two counter-rotating primary recirculations were identified (Lee and Park, 1994; Baik and Kim, 1999; Li et al., 2005). Next, three primary recirculations were found in a street canyon of AR 3.5 (Baik and Kim, 1999). Some of the aforementioned studies also investigated the pollutant dispersion in street canyons. Lee and Park (1994) used an initial, instantaneous pollutant source at the street level to compute the time constant for pollutant dilution. They concluded that the pollutant transport along the streamlines was dominated by advection, while across the streamlines it was dominated by diffusion. (Baik and Kim, 1999) employed a continuous pollutant line source to compute pollutant concentration budget. They showed that the pollutant removal from the street canyon was mainly accomplished by vertical turbulent diffusion.

Recently, the large-eddy simulation (LES) technique has been applied to simulate the turbulent pollutant transport in street canyons. The major merits of LES are its capability of calculating the unsteadiness and intermittency of the flow as well as providing the detailed information on the turbulence structure, which, however, cannot be handled by a k-ε model. Ca et al. (1995) employed a two-dimensional (2D) LES model to study the thermal environment of street canyons and the corresponding impacts on the wind flow. Liu and Barth (2002); Liu et al. (2004) adopted an three-dimensional (3D) LES with a dynamic SGS model to investigate the flow field, pollutant transport, and pollutant removal mechanism in street canyons of AR 0.5, 1, and 2.0 at a Reynolds number of 12,000. Their analysis revealed that the pollutant removal was governed mainly by the roof-level turbulent dispersion on the leeward side. Because of the weaknesses of the conventional k − ε model in handling the transient turbulent transport across the roof level of the street canyon with zero vertical mean flow, it was evident that the LES is more sophisticated for the calculation of the ventilation and pollutant dispersion behaviors. Based on the LES databases accumulated by Liu and Barth (2002) and Liu et al. (2004), Liu et al. (2005) calculated some statistical properties to examine the pollutant distribution, average pollutant concentration and pollutant retention time as well as the air exchange rate (ACH) and pollutant exchange rate (PCH).

Although LES is gaining wider and wider applications in street-canyon pollution research, its demanding requirement in computational resources and highly refined near-wall resolution prohibits its further extension to street canyons of higher AR (≥ 3). In reality, the case of high-rise buildings surrounding narrow street is not rare in crowded cities like Hong Kong and New York. To solve this problem, wall-layer models (Piomelli and Balaras, 2002) are usually adopted in LES models to relieve the heavy computational demand in the near-wall region. In this study, a LES with a wall model was developed for high-aspect-ratio street canyons and validated against measurements. It was then applied to simulate a street canyon of AR 3 and explore the flow field and pollutant dispersion inside the street canyon.

* *Corresponding author address*: Dr. Dennis Y. C. Leung, Department of Mechanical Engineering, The University of Hong Kong, Pokfulam Road, Hong Kong, China; e-mail: ycleung@hku.hk.

2. MATHEMATICAL MODEL

The incompressible turbulence under isothermal condition was considered in this study. The governing equations were the Navier-Stokes and continuity equations. The LES technique was used to calculate the resolved-scale motions by directly solving the filtered governing equations and modeling only the subgrid-scale (SGS) motions. In LES, a spatial filter is applied either explicitly or implicitly to the turbulent flow field. Based on this filtering operation, a variable Φ is decomposed into its resolved-scale component $\overline{\phi}$ and SGS component ϕ' .The large energy-containing resolved-scale component $\overline{\phi}$ is defined mathematically as

$$\overline{\phi}(x_i,t)=\int_\Omega \phi(x_i,t)G(x_i-\xi_i,\overline{\Delta})\,\mathrm{d}\xi_i. \tag{1}$$

Here, G is the filter function, x_i and ξ_i the spatial coordinates in i direction, $\overline{\Delta}$ the filter width, and Ω the spatial domain. This filtering operation involves both flow and scalar transport fields, which are discussed in detail below.

2.1 Flow equations

Applying the spatial filtering operation Eq. (1) to the governing equations yields the dimensionless resolved-scale dynamic equations

$$\frac{\partial\overline{u}_i}{\partial t}+\frac{\partial}{\partial x_j}\overline{u}_i\overline{u}_j=-\frac{\partial\overline{p}}{\partial x_i}-\frac{\partial\tau_{ij}}{\partial x_j}+\frac{1}{\mathrm{Re}}\frac{\partial^2\overline{u}_i}{\partial x_j\partial x_j} \quad \text{and} \tag{2}$$

$$\frac{\partial\overline{u}_i}{\partial x_i}=0, \tag{3}$$

where $\overline{u}_i$ and $\overline{u}_j$ are the resolved-scale velocity components, respectively, in the i and j directions, and $\overline{p}$ is the resolved-scale kinematic pressure. Equations (2) and (3) are expressed in tensor notation so that the indices i and j range over the spatial dimension. The reference length scale H (the building height of the street canyon of AR 1) and the reference velocity scale U (freestream velocity) are employed to make the above equations dimensionless. The Reynolds number is defined as Re = UH/v, where v is the kinematic viscosity of air. The SGS stresses

$$\tau_{ij}=\overline{u_iu_j}-\overline{u}_i\overline{u}_j \tag{4}$$

represent those fluid motions of scales smaller than the filter width. They cannot be calculated explicitly and thus need to be modeled by some SGS models. In this study, the one-equation model (Moeng, 1984; Sullivan et al., 1994) is employed to model the SGS stresses that solves an additional transport equation for the SGS turbulent kinetic energy $k_{sgs}\ (=\overline{u_i'u_i'}/2)$

$$\frac{\partial k_{sgs}}{\partial t}+\overline{u}_i\frac{\partial k_{sgs}}{\partial x_i}=P-\varepsilon+\frac{\partial}{\partial x_i}\left(\frac{2}{\mathrm{Re_T}}\frac{\partial k_{sgs}}{\partial x_i}\right), \tag{5}$$

where

$$P=2\nu_{\mathrm{T}}\overline{S}_{ij}\overline{S}_{ij},\qquad \varepsilon=C_\varepsilon\frac{k_{sgs}^{3/2}}{\ell},$$
$$\ell=(\Delta x\Delta y\Delta z)^{1/3},\qquad \overline{S}_{ij}=\frac{1}{2}\left(\frac{\partial\overline{u}_i}{\partial x_j}+\frac{\partial\overline{u}_j}{\partial x_i}\right), \tag{6}$$
$$\mathrm{Re_T}=\mathrm{UH}/\nu_{\mathrm{T}},\qquad \nu_{\mathrm{T}}=C_k k_{sgs}^{1/2}\ell,$$

and C_k and C_ε are model constants. Li et al. (2007b) applied this model to a turbulent open channel flow and suggested an optimum set of constants C_k = 0.03 and C_ε = 1.0. The SGS stresses are then modeled by the eddy-viscosity assumption in the form

$$\tau_{ij}=-2\nu_{\mathrm{T}}\overline{S}_{ij}. \tag{7}$$

2.2 Wall model

To mitigate the demanding spatial resolution requirement of LES near rigid walls, yet maintain a realistic description of the effects of near-wall processes on the outer flow, a wall model (wall function) is usually adopted. Based on the performance evaluation of different wall models in a periodic channel flow (Temmerman et al. 2003), the 1/7th power law (Werner and Wengle, 1991) is selected in this study to model the fluid motions near the solid boundaries (i.e. ground, walls, and roofs). This wall model is a two-layer approximation and is based on the assumption of a 1/7th power law outside the viscous sublayer, interfaced with the linear profile in the viscous sublayer:

$$u_1^+=\begin{cases} y_1^+ & \text{if } y_1^+\le 11.8\\ 8.3(y_1^+)^{1/7} & \text{if } y_1^+>11.8\end{cases} \tag{8}$$

with $u_1^+=u_1/u_\tau,\ u_\tau=\sqrt{\tau_w/\rho}$ and $y_1^+=y_1u_\tau/\nu$. Here, u_1 is the resolved velocity tangential to the wall at the wall-nearest point, y_1 the distance of this point from the wall, and τ_w the shear stress at the wall.

2.3 Scalar transport equation

Applying the filter to the passive scalar transport equation yields the dimensionless resolved-scale scalar transport equation

$$\frac{\partial\overline{c}}{\partial t}+\frac{\partial}{\partial x_i}\overline{u}_i\overline{c}=-\frac{\partial\sigma_i}{\partial x_i}+\frac{1}{\mathrm{ReSc}}\frac{\partial^2\overline{c}}{\partial x_i\partial x_i}, \tag{9}$$

where $\overline{c}$ is the resolved-scale scalar (pollutant) mixing ratio, Sc = v/D is the Schmidt number, and D is the mass diffusivity. The first term on the right-hand side of Eq. (9) represents SGS turbulent diffusion whose fluxes

$$\sigma_i=\overline{u_ic}-\overline{u_i}\overline{c} \tag{10}$$

are smaller than the filter width and are modeled by the eddy-diffusivity model

$$\sigma_i=-\nu_c\frac{\partial\overline{c}}{\partial x_i}, \tag{11}$$

where the model constant $\nu_c=3\nu_{\mathrm{T}}$ is adopted (Moeng, 1984; Sullivan et al., 1994).

2.4 Numerical method

The resolved-scale dynamic equations are solved by the Galerkin finite element method (GFEM). Trilinear (brick) elements are used to approximate the resolved-scale velocity, pressure, and scalar mixing ratio. The implicit coupling between velocity and pressure in Eqs. (2) and (3) is solved by the second-

order accurate fractional-step method. The advection and diffusion terms in the dynamic equations are integrated in time by the Runge-Kutta and Crank-Nicolson schemes, respectively (Ferziger and Peric, 2002), which are both second-order accurate. The non-overlapping domain decomposition technique and MPI (Gropp and Lusk, 1994) are employed to parallelize the code. The details of the numerical method are discussed by Liu and Leung (2006) and Li et al. (2007b).

2.5 Computational domain and boundary conditions

Figure 1 depicts the schematic diagram of the computational domain of the LES, which represents an idealized 2D street canyon. The spanwise-homogeneous computational domain consists of a street canyon of height h at the bottom and a free surface layer of height 3h over the buildings and street. The spanwise extent of the computational domain is L. This geometrical configuration represents an idealized street canyon of width b between the leeward and windward buildings of equal height *h*. The free surface layer extends b_u and b_d in length in the upstream and downstream directions, respectively.

The prevailing wind flow is simulated in the form of pressure-driven free stream in the free surface layer only. No large-scale pressure force is prescribed inside the canyon. To investigate the worst scenario of street-canyon air pollution, the approaching wind is set to be perpendicular to the street axis, which results in a free-stream wind speed U in the streamwise direction. The wind flow is periodic in both the streamwise direction in the free surface layer and the spanwide direction of the whole domain. This flow configuration represents infinitely long street canyons in the spanwise direction that are repeated infinitely in the streamwise direction.

The vehicular pollutant is simulated by a ground-level continuous scalar line source measuring L in length placed parallel to the street axis at a distance x_s(= 0.5*h*) from the leeward building. A passive and inert gaseous pollutant is considered whose total emission rate is Q. In the free surface layer, the upstream inlet is prescribed as free of pollutants, while an open boundary condition for the pollutant

$$\frac{\partial \overline{c}}{\partial t} + \overline{u}\frac{\partial \overline{c}}{\partial x} = 0 \qquad (12)$$

is used at the downstream outlet. Equation (12) allows the pollutant to leave the computational domain through the downstream outlet without obvious distortion. The von Neumann (zero normal gradient) conditions for the pollutants are set on all the solid boundaries. A periodic boundary condition for the pollutant is applied in the spanwise direction, which is the same as its flow counterpart.

3. MODEL VALIDATION

The reliability of the current LES model is evaluated by comparing the results of street canyons of AR 1 and AR 2 with those obtained by previous numerical models and experiment (Li et al., 2007a). The Reynolds number of this LES is around 15,000, which is slightly higher than that of the previous numerical and experimental studies.

3.1 Flow field

Figure 2 compares the vertical profiles of velocities and their fluctuations inside the street canyon of AR 1 by different numerical models and experiment. A good agreement among all the mean velocity components (Fig. 2a and b) is shown inside the canyon (z/H < 1). For the velocity fluctuations (Fig. 2c and d), the results from the numerical models and experiment generally agree well with each other. Their peak values locate slightly above the roof level while the values are nearly constant at the core region. Above the canyon (z/H > 1), the velocity fluctuations show an obvious discrepancy between different results. This discrepancy is mainly due to the different configurations adopted in the numerical models and experiment. In the experiment (Li et al., 2007a), a height of 3H was extended above the buildings to simulate the free surface layer, which is the same as that in the current LES calculation. The length of the street in the experiment is limited (about 3h), however, in the current LES, the street is infinitely long due to the periodic boundary conditions used in the spanwise direction. Besides, the side walls of the water channel experiment would impose some end-wall effects on the fluctuations.

Figure 2 also illustrates the properties of grid dependence of the current LES calculation. A fine mesh without the wall model and a coarse mesh with the wall model were used to calculate the same problem that gave consistent results. It is thus suggested that the meshes adopted in the current LES is fine enough to output grid-independent results. Figure 3 compares the vertical profiles of velocities and their fluctuations at several locations in the street canyon of AR 2 by different models and experiment. Similar to the street canyon of AR 1, the mean velocity components (Fig. 3a and b) inside the canyon (z/H < 2) show good agreement while the fluctuations (Fig. 3c and d) show a relatively large discrepancy between different models. The velocity fluctuations calculated by the current LES show some resemblance with those obtained from experiment, but with a smaller magnitude. This may partly attribute to the end-wall effects described above. Moreover, the complicated recirculating wind flow in the street canyon of AR 2 may contribute to this discrepancy (Li et al., 2007a).

Conclusively, the current LES model gives reasonably good results for velocity and fluctuation calculation in street canyons of AR 1 and 2. Whereas, there are some discrepancies between the numerical and experimental results. The possible explanation may be the different averaging method adopted in the LES calculation and water channel experiment. In the LES, the flow quantities are averaged both temporally and spatially (along the spanwise direction). In the

experiment, the flow quantities were only measured at the vertical center plane. In addition, to simulate the urban atmospheric boundary layer, the free stream flow was perturbed by placing some vortex generators upstream, which make the incoming flow higher in turbulence intensities. On the contrary, in our LES, turbulence was generated solely by mechanical shear, which certainly produces less turbulence in street canyons compared with that in the water channel experiment. Other than these differences, the current LES employs the same values of model constants throughout the computational domain, which may not fully account for the variance of flow characteristics everywhere in the domain. Some dynamic processes have been proposed and tested for the one-equation model (Menon and Kim, 1996; Krajnovic et al., 1999; Krajnovic and Davidson, 2001), however, this dynamic process will unavoidably increase the computational load tremendously. Therefore, in this study, a compromise between accuracy and cost is made.

3.2 Scalar field

Figure 4 shows the dimensionless mean pollutant mixing ratio <c>UHL/Q on the leeward and windward facades of the street canyon of AR 1 calculated by the current LES and measured by previous wind tunnel experiments (Pavageau, 1996; Meroney et al., 1996; Pavageau and Schatzmann, 1999). The current LES calculations with different spatial resolutions output consistent results at most places except at the ground-level corners, where the coarse mesh calculation with wall model underpredicts the pollutant mixing ratio for 20% to 30%. It is worth mentioning that the coarse mesh calculation utilizes a very coarse grid resolution, especially in the near-wall region. The overall underprediction is partly caused by the coarse grid used in the LES. Moreover, the different configurations of the calculation and the experiments, as mentioned in the previous sections, may lead to the differences. In the experiments, the locations of measurement points for the pollutant mixing ratio in the proximity of walls are critical because of the sharp pollutant gradient.

The spatial distribution of the calculated (with coarse mesh and wall model) dimensionless pollutant mixing ratio and its variance <c″c″>$(UHL/Q)^2$ is depicted in Fig. 5. The calculated pollutant mixing ratio (Fig. 5a) agrees well with the previous wind-tunnel measurements of Pavageau and Schatzmann (1999) (Fig. 5b). However, as explained above, the current LES slightly underpredict the pollutant mixing ratio at the ground-level corners due to the coarseness of the spatial resolution used. The calculated pollutant mixing ratio variance (Fig. 5c) also agrees well with the wind-tunnel measurements at most locations. Because of the rapid mixing processes in the vicinity of the line source, large gradients of pollutant mixing ratio and variance are observed at the ground level. A local maximum of pollutant mixing ratio variance is developed at the roof level. The calculated results suggest that its location is slightly upstream. In contrast, the measurements show that it spans nearly over the whole breadth of the street. The current LES also underpredicts the pollutant mixing ratio variance there mainly due to the underpredicted roof-level turbulence intensity.

4. RESULTS AND DISCUSSIONS

In this section, we apply the LES with wall model to street canyon of AR 3 to examine the wind flow and pollutant dispersion behaviors in a high-aspect-ratio street canyon. For the street canyons of AR 1 and 2, these behaviors have been discussed in detail in Liu and Barth (2002); Liu et al. (2004); Li et al. (2005). In the following sections, brackets < > represent the spanwise and temporal averages of the flow and turbulence properties, while ″ represents the deviation from these averages.

4.1 Characteristics of flow field

To illustrate the wind flow structure in the street canyon of AR 3, the streamfunction ψ, which is defined as

$$\frac{\partial \psi}{\partial z} = \langle \overline{u} \rangle \quad \text{and} \quad -\frac{\partial \psi}{\partial x} = \langle \overline{w} \rangle \,, \tag{13}$$

,is depicted in Fig. 6 in which a positive (negative) streamfunction indicates counter-clockwise (clockwise) rotating recirculation. Three vertically-aligned primary recirculations are developed in the street canyon. The upper and lower ones are clockwise rotating and the middle one is counter-clockwise rotating. The roof-level wind flow is similar to that in street canyons of AR 1 and 2 (Liu et al., 2004; Li et al., 2005).

The upper recirculation ($1.9 < z/H < 3.0$) is mainly driven by the shear force of the prevailing wind flow. It then induces the relatively weaker middle primary recirculation ($0.7 < z/H < 1.9$) through shear force. A very weak primary recirculation at the bottom is eventually created by the middle recirculation. The magnitude of the minimum streamfunction of the upper recirculation $\psi = -0.03$ is about 4 times of the maximum streamfunction of the middle recirculation $\psi = 0.008$, and is 30 times of the magnitude of the minimum streamfunction of the lower recirculation. This weak lower recirculation is mainly due to the sharp decrease of shear force transfer between the primary recirculations. This phenomenon is discussed again based on the spatial variation of the streamwise and vertical mean velocities in the upcoming sections. Similar to the cases of street canyons of AR 1 and 2, weak counterclockwise-rotating secondary recirculations are developed in the upper leeward corner and ground-level corners.

Figure 7a and b shows the spatial variation of the dimensionless mean wind velocities <u> and <w>, respectively. The pattern of streamwise velocity in the street canyon can be divided vertically into four layers, separated by contour values of zero. In the first and third layer (counting from roof level downward to ground level), the wind flows toward the windward

building, while in the other two layers, the wind flows toward the leeward building. Similarly, the pattern of vertical velocity in the street canyon can be divided vertically into three layers. In each layer, the wind flows in opposite directions (upward or downward) near the opposite buildings, corresponding to the three primary recirculations depicted in the streamfunction (Fig. 6). At the ground level, the wind blows upward with a very small speed (around 0.5% of the freestream value), which is unable to dilute the pollutants emitted there. The wind speed, both streamwise and vertical, decreases sharply with decreasing height in the street canyon. This sharp change will reduce the amount of pollutant being removed by the advection, resulting in even worse air quality in the street canyon of AR 3 than those in street canyons of AR 1 and 2.

To further examine the turbulence characteristics in the street canyon, the dimensionless velocity fluctuations $<u''u''>/U^2$ and $<w''w''>/U^2$ (Fig. 7c and d) are analyzed. The streamwise velocity fluctuation exhibits a local maximum of 0.01 at the roof-level leeward corner. Another local maximum of 0.002 appears near the leeward building at about z/H = 2.0, coinciding with the interface between the upper and middle primary recirculations. At the ground level, the streamwise velocity fluctuation is only 0.01% of the roof-level maximum. The vertical velocity fluctuation has a maximum of 0.004 at the roof-level windward corner, whose value is only half of its streamwise counterpart. Another local maximum of vertical velocity fluctuation (0.002) is developed near the windward building at about z/H = 2.0. This maximum located at the same level of one of the streamwise maxima. These observations can be explained through the mechanism of turbulent kinetic energy (TKE) production. At the roof level, the local maximum of velocity fluctuations are produced by the mechanical wind shear and Reynolds stress between the free stream flow and the upper clockwise-rotating primary recirculation. These interactions, in the form of velocity gradient, convert the mean kinetic energy into TKE. The TKE is then carried downward into the street canyons following the recirculations. Other two local maxima are created by the interactions between the upper and middle primary recirculations. Their small magnitudes are due to the relatively weaker wind shear compared with the free stream flow. No local maximum is found at the interface of the middle and lower recirculations because the lower recirculation is too weak, as noted above, to create any local maximum of velocity fluctuations.

Conclusively, the flow pattern in the street canyon of AR 3 is more complicated than that found in the street canyons of AR 1 and 2. Both the velocities and turbulence intensities exhibit a common feature of decreasing strength with decreasing height which further deteriorates the air quality.

4.2 Characteristics of pollutant dispersion

As described in Liu et al. (2004), the pollutant fllows the recirculation in general. However, some distinct features are observed in pollutant dispersion inside the street canyon of AR 3, which are discussed in this section.

The spatial distributions of the mean pollutant mixing ratio and its variance are shown in Fig. 8. Generally, the air pollutant follows the primary recirculations after being emitted at the ground level. From the roof level down to the ground level, the patterns of the pollutant mixing ratio and its variance can be divided into three layers, roughly corresponding to the three layers of the mean vertical velocities as described in the last section. Within each layer, high pollutant concentrations and variances are generally found at locations where wind flows upward. This phenomenon is mainly due to the fact that the upward wind tends to transport pollutants upwards to the roof level by advection. However, owing to the isolation nature of individual primary recirculations, the upward moving pollutants are hindered by the primary recirculation or the free stream flow just above it. A small portion of these upward-moving pollutants is then transported to the primary recirculation or the free surface layer above through turbulent dispersion. The remaining small portion of these pollutants is transported back into the street canyon by the downward wind flow through advection. Hence, a large amount of pollutants is accumulated near the buildings where wind flows upward.

Large pollutant concentration and variance gradients are observed not only in the wake of pollutant line source, but also at the interfaces of primary recirculations and/or free surface layer, specifically near the points (x/H, z/H) = (0, 1.0), (1.0, 2.25), and (0, 3.0). These findings suggest that when performing field or laboratory measurements, one must pay attention to, in addition to the wake of the line source, the rapid changes of wind flow and pollutant quantities at these critical points. Also, these large gradients indicate that there are intensive turbulent dispersion processes nearby. The pollutants emitted from the line source are thus transported from one primary recirculation to another, until removed from the street canyon, by means of advection and turbulent dispersion. As a result, the efficiency of the pollutant removal depends mainly on two factors: the first one is the local wind speed, especially the vertical one, which is responsible for transporting pollutants upward to the roof level through advection; the other one is the intensity of turbulent dispersion, which is responsible for transferring pollutants between primary recircultions and/or the free surface layer. In the street canyon of AR 3, the vertical velocity near the ground level is very small (Fig. 7b), thus the advection is very weak and the pollutant mixing ratio near the ground level is at least an order of magnitude greater than other places within the street canyon.

5. CONCLUSIONS

In this study, an LES model was developed

based on a one-equation SGS model and finite element method for incompressible flow. A 1/7th wall model was implemented in this LES near the rigid walls to mitigate the near-wall resolution requirement. This LES model was applied to calculate the flow field and pollutant dispersion in street canyons of AR 1 and 2, and the calculated results were validated against several laboratory experiments. The validation showed that the current LES model could output reliable velocity and fluctuation results compared to water channel experiment. The pollutant mixing ratio and its variance calculated by the current LES were also compared favorably with wind tunnel measurements. It was shown that the current LES model was capable of handling both the flow field and pollutant transport inside street canyons.

The validated LES model was then employed to calculate the street canyon of AR 3. It was shown that three vertically-aligned primary recirculations were formed inside the street canyon. These recirculations showed decreasing strength with decreasing height. The magnitude of the mean velocities near the ground level was only 0.5% of the free stream velocity, which makes the pollutant emitted at the ground level very difficult to be transported towards the roof level. Some local maxima of the turbulence intensities were found at the interface between the free surface layer and the upper primary recirculation and the interface between the upper and middle primary recirculations.

A passive and inert gaseous pollutant emitted from a line source along the centerline of the street at the ground level was simulated. It was found that the pollutant followed the trajectories of the primary recirculations. High pollutant concentration and variance were found near the buildings where wind flowed upward. Moreover, large gradient of pollutant concentration and variance were found at the interfaces between the primary recirculations and/or the free surface layer. These findings can serve as a general principle applying to street canyons of higher aspect ratio. They can also help to make appropriate arrangements when performing laboratory or field measurement of pollutant transport.

ACKNOWLEDGEMENTS

The authors wish to acknowledge the Hong Kong Research Grant Council for supporting this project under grants HKU 7196/03E and 7111/04E. The authors would like to thank Computer Centre, The University of Hong Kong for accessing their high performance cluster. The financial support from the CRCG Conference/Travel Grant of HKU for the first author to attend this conference is also acknowledged.

REFERENCES

Baik, J.-J., Kim, J.-J., 1999. A numerical study of flow and pollutant dispersion characteristics in urban street canyons. Journal of Applied Meteorology 38, 1576–1589.

Ca, V. T., Asaeda, T., Ito, M., Armfield, S., 1995. Characteristics of wind field in a street canyon. Journal of Wind Engineering and Industrial Aerodynamics 57 (1), 63–80.

DePaul, F., Sheih, C., 1986. Measurements of wind velecities in a street canyon. Atmospheric Environment 20, 455–459.

Ferziger, J. H., Peri´c, M., 2002. Computational Methods for Fluid Dynamics, 3rd Edition. Springer, Berlin.

Gropp,W., Lusk, E., 1994. User's guide for mpich, a portable implementation of MPI. Technical Report ANL-96/6, Argonne National Laboratory.

Huang, H., Akutsu, Y., Arai, M., Tamura, M., 2000. A two-dimensional air quality model in an urban street canyon: evaluation and sensitivity analysis. Atmospheric Environment 34, 689–698.

Johnson, G. T., Hunter, L. J., 1995. A numerical study of dispersion of passive scalars in city canyons. Boundary-Layer Meteorology 75, 235–262.

Krajnovi´c, S., Davidson, L., 2001. Large eddy simulation of the flow around a three-dimensional bluff body. AIAA paper 01-0432.

Krajnovi´c, S., M¨uller, D., Davidson, L., 1999. Comparison of two one-equation subgrid models in recirculating flows. In: Voke, P. R., Sandham, N. D., Kleiser, L. (Eds.), Direct and Large-Eddy Simulation III. Kluwer, Netherlands, pp. 63–74.

Lee, I. Y., Park, H. M., 1994. Parameterization of the pollutant transport and dispersion in urban street canyons. Atmospheric Environment 28, 2343–2349.

Li, X.-X., Leung, D. Y. C., Liu, C.-H., Lam, K. M., 2007a. Physical modeling of flow filed inside urban street canyons. Submitted to Journal of Applied Meteorology and Climatology.

Li, X.-X., Liu, C.-H., Leung, D. Y. C., 2005. Development of a k−ε model for the determination of air exchange rates for street canyons. Atmospheric Environment 39 (38), 7285–7296.

Li, X.-X., Liu, C.-H., Leung, D. Y. C., Lam, K. M. (2006), "Recent progress in CFD modeling of wind field and pollutant transport in street canyons", Atmospheric Environment 40, 5640-5658.

Li, X.-X., Liu, C.-H., Leung, D. Y. C., 2007b. Development of an FEM LES with one-equation subgrid-scale model for incompressible flow. Submitted to Computer Methods of Applied Mechanics and Engineering.

Liu, C.-H., Barth, M. C., 2002. Large-eddy simulation of flow and scalar transport in a modeled street canyon. Journal of Applied Meteorology 41 (6), 660–673.

Liu, C.-H., Barth, M. C., Leung, D. Y. C., 2004. Large-eddy simulation of flow and pollutant transport in street canyons of different building-height-to-street-width ratios. Journal of Applied Meteorology 43, 1410–1424.

Liu, C.-H., Leung, D. Y. C., 2006. Finite element solution to passive scalar transport behind line sources under neutral and unstable stratification. International Journal for Numerical Methods in Fluids 50 (5), 623–648.

Liu, C.-H., Leung, D. Y. C., Barth, M. C., 2005. On the

prediction of air and pollutant exchange rates in street canyons of different aspect ratios using large-eddy simulation. Atmospheric Environment 39, 1567–1574.

Menon, S., Kim, W. W., 1996. High Reynolds number flow simulations using the localized dynamic subgrid-scale mode. AIAA paper 96-0425.

Meroney, R. N., Pavageau, M., Rafadalis, S., Schatzmann, M., 1996. Study of line source characteristics for 2D physical modelling of pollutant dispersion in street canyons. Journal of Wind Engineering and Industrial Aerodynamics 62, 37–56.

Moeng, C. H., 1984. A large-eddy-simulation model for the study of planetary boundary-layer turbulence. Journal of the Atmospheric Sciences 4 (13), 2052–2062.

Nakamura, Y., Oke, T. R., 1988. Wind, temperature, and stability conditions in an east-westoriented urban canyon. Atmospheric Environment 22, 2691–2700.

Oke, T. R., 1988. Street design and urban canopy layer climate. Energy and Buildings 11, 103–113.

Pavageau, M., 1996. Concentration fluctuations in urban street canyons - groundwork for future studies. Technical report, Meteorological Institute of the University of Hamburg, 97 pp.

Pavageau, M., Schatzmann, M., 1999. Wind tunnel measurements of concentration fluctuations in an urban street canyon. Atmospheric Environment 33, 3961–3971.

Piomelli, U., Balaras, E., 2002. Wall-layer models for large-eddy simulations. Annual Review of Fluid Mechanics 34, 349–374.

Sullivan, P. P., McWilliams, J. C., Moeng, C. H., 1994. A subgrid-scale model for large-eddy simulation of planetary boundary-layer flows. Boundary-Layer Meteorology 71 (3), 247–276.

Temmerman, L., Leschziner, M. A., Mellen, C. P., Fro¨ohlich, J., 2003. Investigation of wallfunction approximation and subgrid-scale models in large eddy simulation of separated flow in a channel with streamwise periodic constrictions. International Journal of Heat and Fluid Flow 24, 157–180.

Werner, H., Wengle, H., 1991. Large-eddy simulation of turbulent flow over and around a cube in a plate channel. In: 8th Symposium on Turbulent Shear Flows. pp. 155–168.

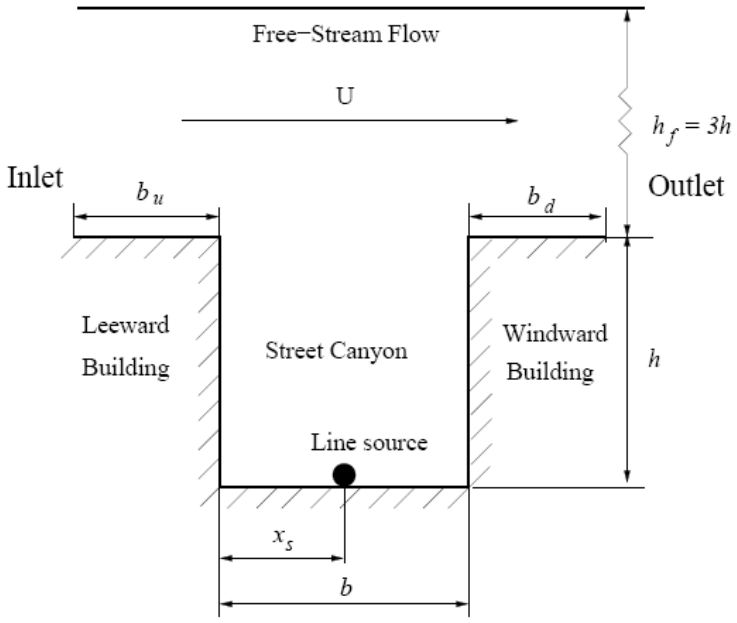

Fig. 1. Schematic diagram of computational domain for the flow and pollutant transport in a street canyon.

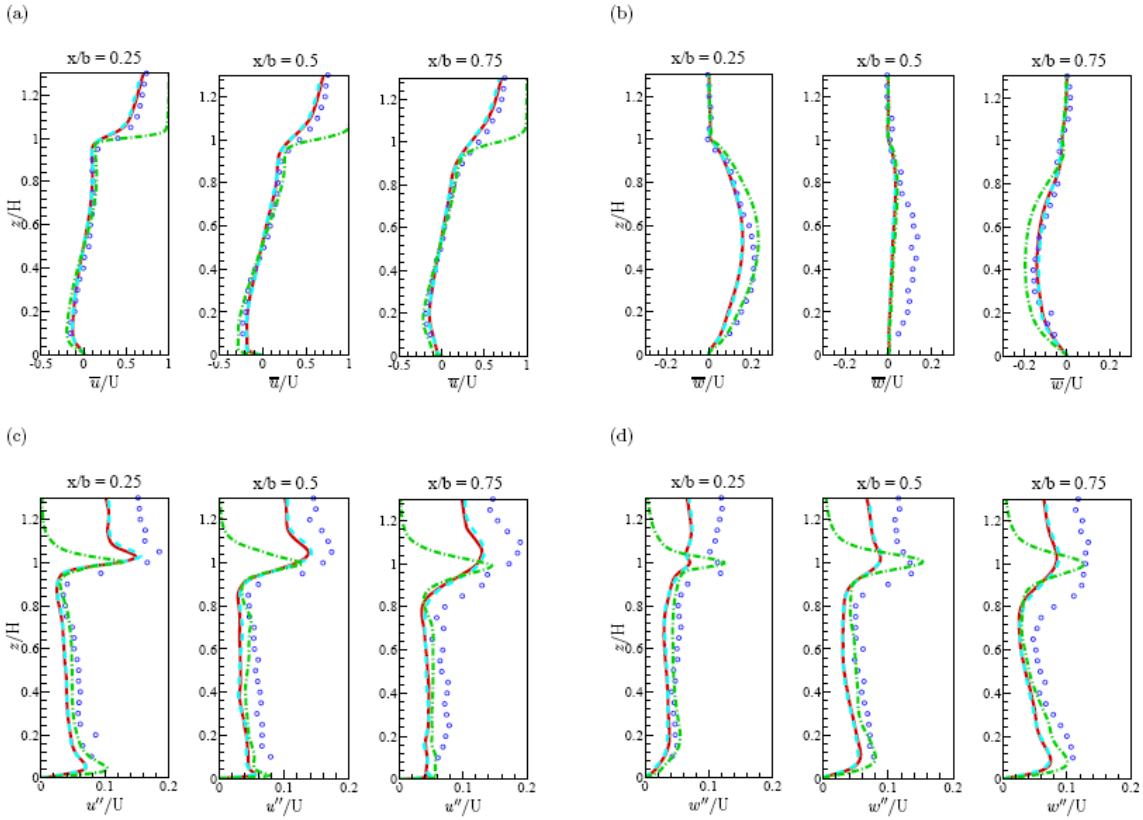

Fig. 2: Comparison of vertical profiles in unity street canyon by different models and experiment. ———: Calculation by the current LES model with fine mesh; − − −−: Calculation by the current LES model with coarse mesh and wall model; − · − · −: Calculation by LES (Liu et al., 2004); O: Water-channel experiment (Li et al., 2007a).

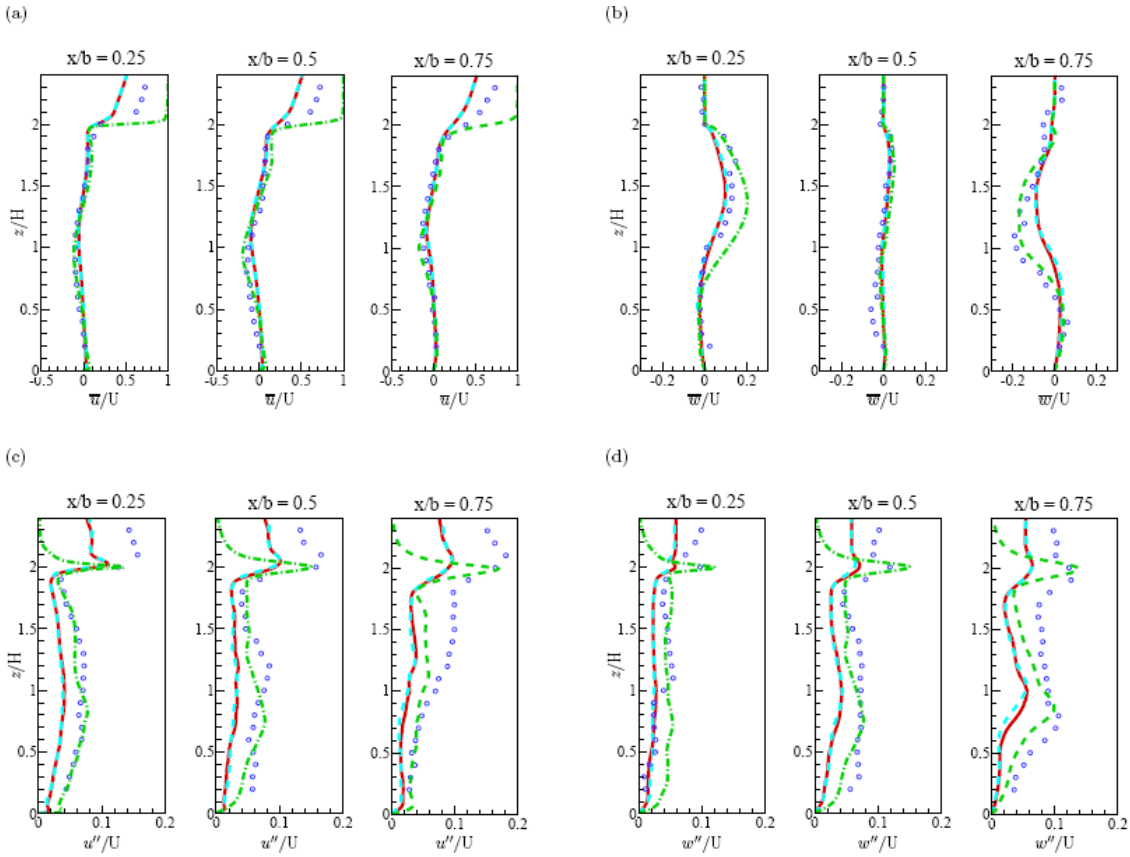

Fig. 3: Comparison of vertical profiles in street canyon of AR 2 by different models and experiment. Lines and symbols carry the same meanings as in Fig. 2.

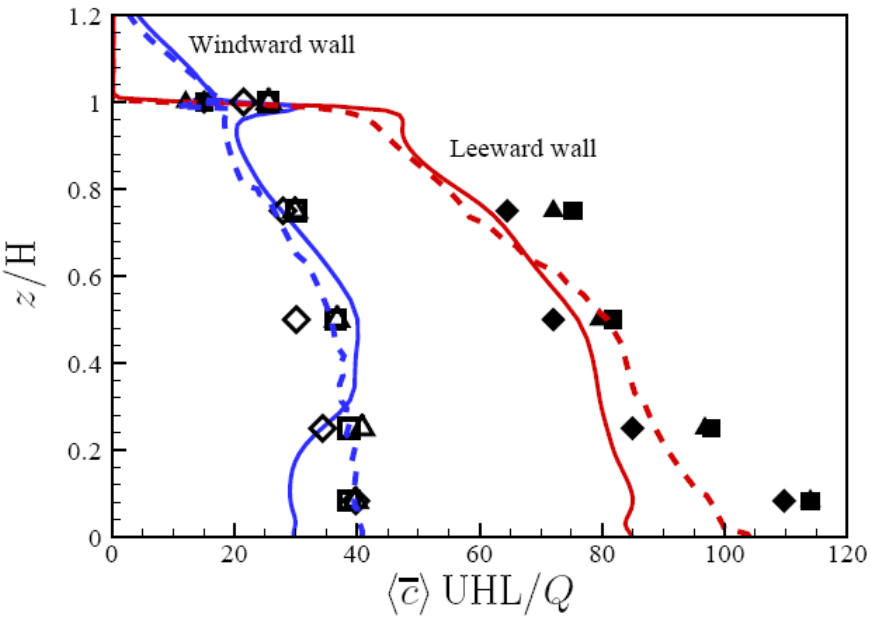

Fig. 4: Dimensionless mean pollutant mixing ratio <c>UHL/Q on the leeward and windward walls of the unity street canyon. Calculated values are ———: by coarse mesh with wall model and − − −−: by fine mesh. Measured values on the windward walls are □: Pavageau (1996), ◊: Meroney et al. (1996) and □: Pavageau and Schatzmann (1999). Filled symbols represent the corresponding values on the leeward wall.

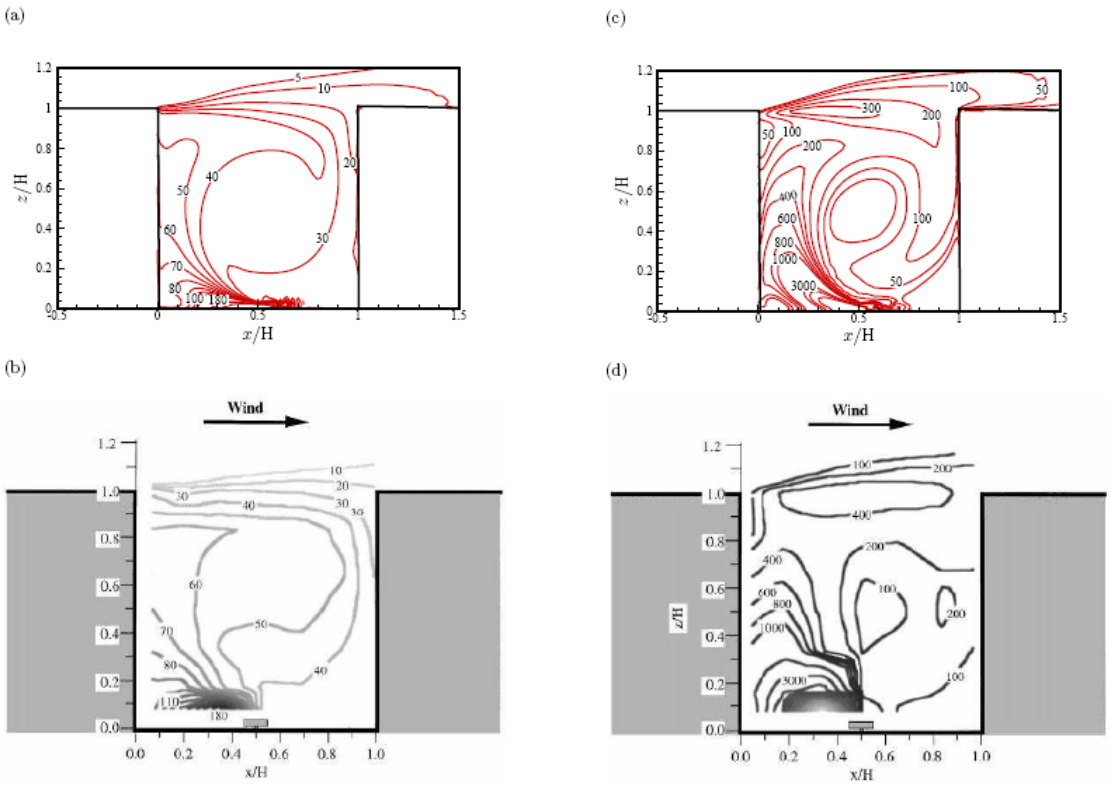

Fig. 5: Spatial distribution of dimensionless mean pollutant mixing ratio and its variance in the unity street canyon. Dimensionless mean pollutant mixing ratio <c>UHL/Q by (a) current LES with coarse mesh and wall model; (b) Pavageau and Schatzmann (1999); and dimensionless mean pollutant mixing ratio variance <c″c″> $(UHL/Q)^2$ by (c) current LES and (d) Pavageau and Schatzmann (1999).

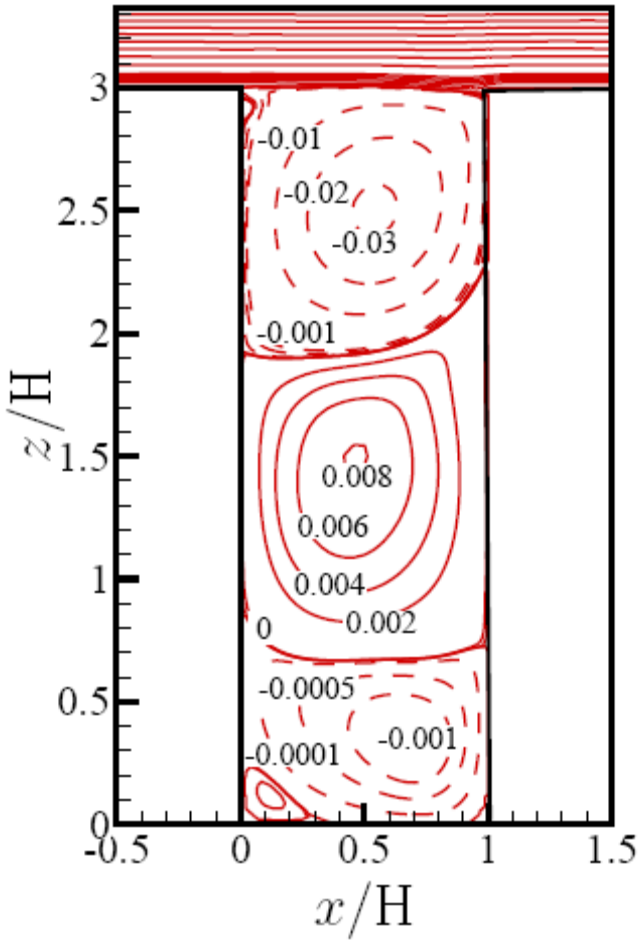

Fig. 6: Spatial distribution of the dimensionless Streamfunction in the street canyon of AR 3.

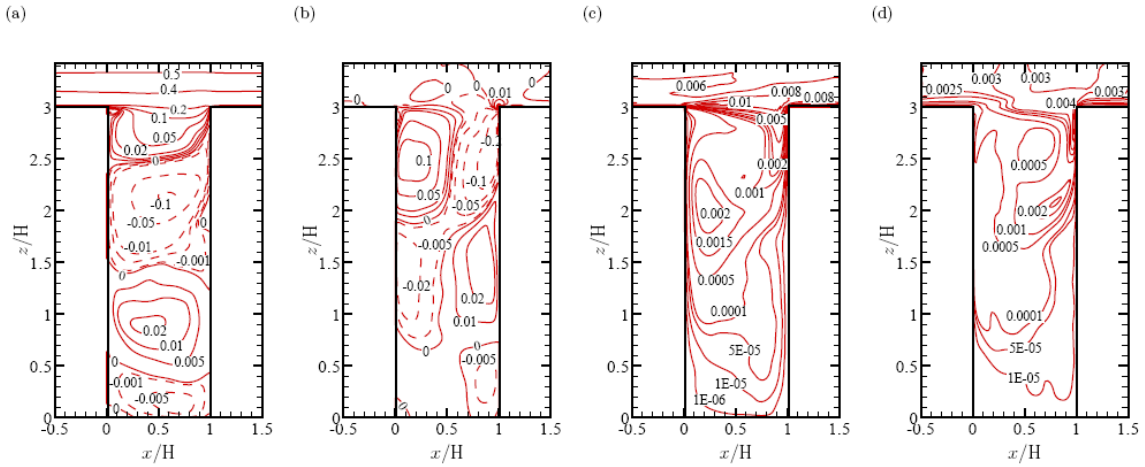

Fig. 7: Spatial distribution of dimensionless mean velocities and fluctuations in the street canyon of AR 3 calculated by current LES. (a) <u> /U; (b) <w>/U; (c) <u″u″> /U^2; (d) <w″w″> /U^2.

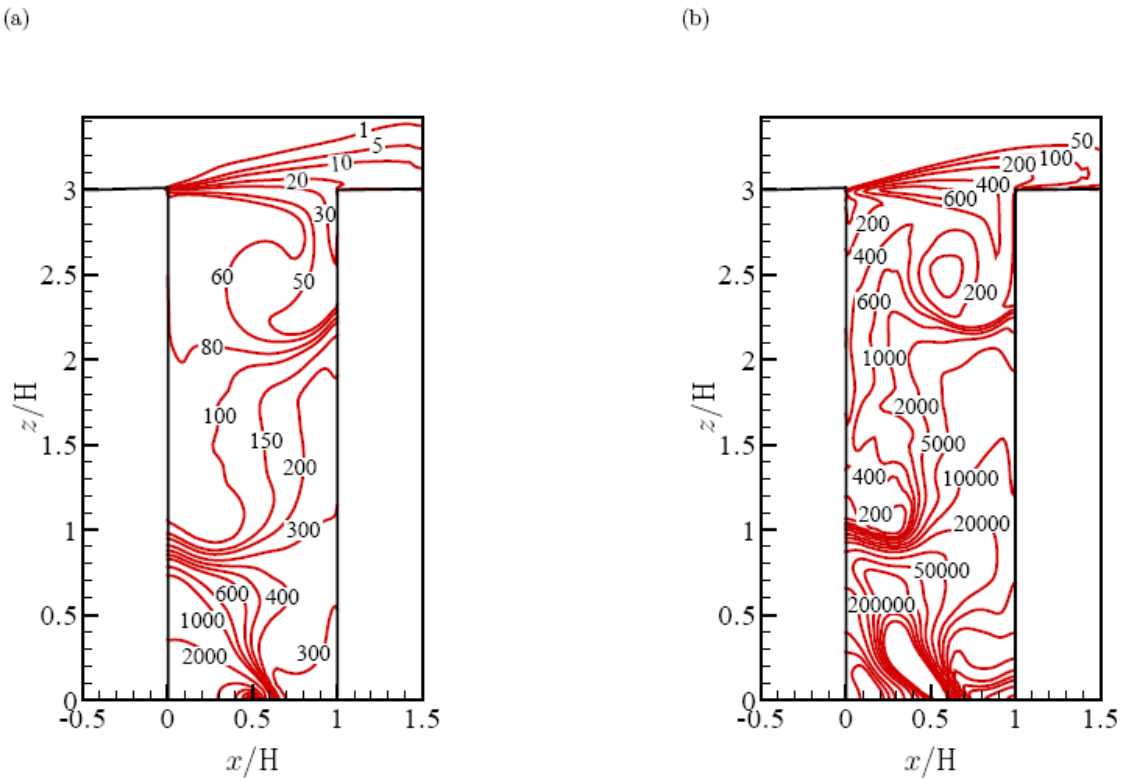

Fig. 8: Spatial distribution of dimensionless mean pollutant mixing ratio and its variance in the street canyon of AR 3 calculated by the current LES. (a) scalar mixing ratio <c>UHL/Q; (b) scalar mixing ratio variance <c″c″> $(UHL/Q)^2$.